

Real Gas Corrections for High Beta Ratio ($\beta > 0.25$) Critical Flow Venturi (CFV) Installations

Aaron N. Johnson
NIST 100 Bureau Drive,
Gaithersburg, MD 20899, USA
Aaron.Johnson@nist.gov

Eric Lemmon
NIST 325 Broadway Street,
Boulder, CO 80305, USA
Eric.Lemmon@nist.gov

NOMENCLATURE

Variables	
a	Speed of sound
A	Cross-sectional area of CFV
β	Beta Ratio = d/D
C^*	Critical flow function
$C_{d,flow}$	CFV flow discharge coefficient
$C_{d,real}$	CFV real gas discharge coefficient = \dot{M}_{real}/\dot{m}_b
c_p	Specific heat at constant pressure per mass
d	Diameter of the CFV throat
D	Diameter in the upstream approach
h	Specific enthalpy per mass
h_t	Total enthalpy per mass = $h + u^2/2$
\mathcal{M}	Molar mass
\dot{m}	Actual CFV mass flow = $C_{d,flow}C_{d,real}\dot{m}_b$
\dot{m}_b	Baseline mass flow derived for ideal flow and ITM thermodynamic model
\dot{M}_{real}	Inviscid mass flow for a real gas
Ma	One dimensional Mach number = u/a
n	Isentropic exponent
P	Pressure
P_b	Back pressure
Pr	Prandtl number
R_f	Recovery factor
R_{univ}	Universal gas constant
r	Dimensionless grouping of thermodynamic variables assumed constant in deriving stagnation temperature using the polytropic model
s	Specific entropy per mass
T_{m1}	Temperature measured by the probe in the approach piping
u	Axial velocity in approach pipe or CFV

u_1	Velocity in the approach pipe upstream of CFV inlet
Z	Compressibility factor
γ	Ratio of specific heats
κ	Exponent in analytic expression of stagnation temperature for polytropic model
ρ	Density

Subscripts	
0	Stagnation condition
1	Static condition in approach piping upstream of CFV inlet
i	Ideal gas
ITM	Ideal thermodynamic model
JM	Johnson method for real gas
p	Polytropic model
RGM	Real gas model
x	Axial distance upstream from the CFV throat

Superscripts	
*	Conditions at CFV throat for $Ma = 1$

ABSTRACT

For almost 50 years, flow measurement applications using critical flow venturis (CFVs) have relied exclusively on the critical flow function (C^*) to correct for real gas effects. This work shows that C^* does not account for all real gas effects. For high beta ratio ($\beta > 0.25$) CFV installations, real gas effects can result in significant mass flow errors even after C^* corrections have been made. These errors are attributed to the idealized thermodynamic models (ITMs) used to calculate the stagnation temperature and pressure. The errors in the stagnation temperature and pressure cause errors in C^* , and ultimately in the CFV mass flow. For methane gas the mass flow errors exceeded 0.1 % for $\beta = 0.5$ at 10 MPa, and are larger than 0.3 % for $\beta = 0.6$ at 20 MPa. For CFVs these errors are comparable with the uncertainty of the flow measurement. This manuscript presents a model that compensates for all real gas effects for β up to 0.6. Comparisons of the real gas model (RGM) and the idealized thermodynamic models (ITMs) are shown for methane up to 20 MPa. We incorporated this new model into the REFPROP thermodynamic program so that real gas corrections can be applied to any user defined gas. We expect that this new model will enable high beta ratio CFV installations to be used reliably at lower uncertainty in circumstances where a low beta ratio is not practical or is undesirable for temperature measurement uncertainty reasons.

1. INTRODUCTION

For more than 50 years critical flow venturis (CFVs) have been used to measure gas mass flow. In the early 1960's researchers realized that accurate mass flow measurements required real gas corrections. Johnson introduced the real gas critical flow factor (C_{JM}^*)¹ to correct the CFV mass flow model for real gas effects [1 - 4]. This thermodynamic property has been considered to be the only correction factor needed to account for real gas effects in CFV flows. Herein we show that C_{JM}^* alone does not compensate for all real gas effects. The stagnation pressure (P_0) and temperature (T_0) also require real gas corrections in high beta ratio CFV installations whenever real gas effects are significant.

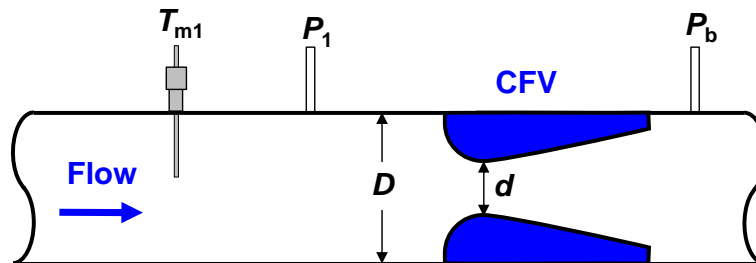


Figure 1. Typical CFV installation where d and D are the respective diameters at the CFV throat section and at the pipe section upstream of the CFV inlet. The ratio of these diameters is the beta ratio $\beta \equiv d/D$, and T_{m1} and P_1 are the measured temperature and pressure in the approach piping.

Figure 1 shows a CFV with a throat diameter of d installed in a pipeline of diameter D . When the ratio of the downstream static pressure to upstream stagnation pressure (P_b/P_0) is less than the critical back pressure ratio, the gas in the upstream piping accelerates through the convergent section of the CFV and reaches sonic velocities at the throat section (*i.e.*, minimum cross sectional area). Pressure waves downstream of the CFV throat section cannot propagate upstream of the sonic throat. Hence, for operating conditions where P_b/P_0 is maintained below the critical ratio,

¹ The subscript "JM" indicates Johnson's Method.

the mass flow is independent of P_b . For a given gas composition the mass flow depends on the measured temperature (T_{m1}) and pressure (P_1) in the approach piping upstream of the CFV throat (see Fig. 1). These measurements of T_{m1} and P_1 are converted into the stagnation temperature (T_0) and pressure (P_0) with the use of a thermodynamic equation of state and the beta ratio ($\beta \equiv d/D$). Low uncertainty T_0 and P_0 are important since the CFV mass flow directly depends on these parameters.

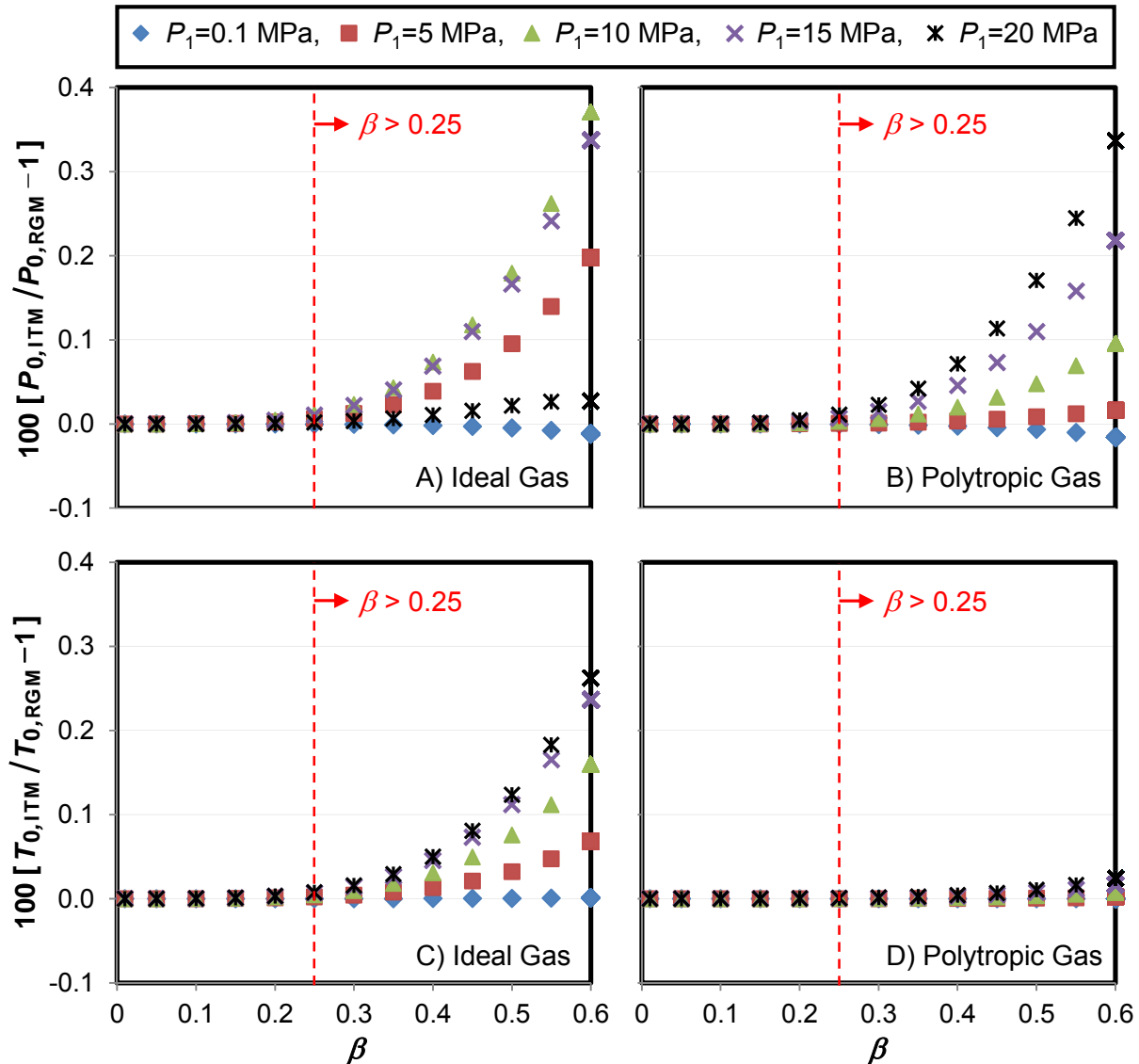


Figure 2. Real gas errors in $P_{0,ITM}$ and $T_{0,ITM}$ plotted versus β . Plots are for methane gas at 295 K for 5 pressures ranging from 0.1 MPa to 20 MPa.

The stagnation temperature and pressure account for the bulk kinetic energy of the flowing gas and therefore differ from the measured temperature and pressure. In CFV applications the stagnation conditions have historically been calculated for a specified gas composition based on T_{m1} , P_1 , and β with either of two idealized thermodynamic models (ITMs): 1) the ideal gas model,

or 2) the polytropic gas model. When $\beta > 0.25$ and real gas effects are significant, errors in T_0 and P_0 based on the ITMs can become significant relative to the CFV measurement uncertainty. In these cases, real gas corrections must be applied to T_0 and P_0 for accurate flow measurements.

The four plots in Fig. 2 show the percent error in $P_{0,ITM}$ and $T_{0,ITM}$ versus β . Here, $P_{0,ITM}$ and $T_{0,ITM}$ are the stagnation pressure and temperature calculated using the ITMs, and $P_{0,RGM}$ and $T_{0,RGM}$ are the stagnation pressure and temperature calculated using the Real Gas Model (RGM) introduced in this manuscript. The Real Gas Model is developed in Section 4 and analytic expressions for $P_{0,ITM}$ and $T_{0,ITM}$ are given in the Appendix. Errors associated with the ideal gas stagnation pressure and temperature are shown in Figs. 2A and 2C, and the corresponding errors for the polytropic gas model are in Figs. 2B and 2D. The results in Fig. 2 are computed for methane gas at 295 K for five pressure isobars ranging from 0.1 MPa to 20 MPa. These plots show that errors in $P_{0,ITM}$ and $T_{0,ITM}$ are negligible when $\beta \leq 0.25$, but can become significant for $\beta > 0.25$. The errors at large β is why documentary standards require $\beta \leq 0.25$ [5, 6]. As expected, the maximum error along each isobar occurs at the maximum beta ratio of $\beta = 0.6$. Errors in $P_{0,ITM}$ nearly reach 0.4 % for both the ideal gas and polytropic model. However, the maximum error for the polytropic model increases monotonically and reaches its maximum value at 20 MPa while the error for the ideal gas model reaches a maximum value at 12 MPa and decrease at increasing pressures up to 20 MPa. The errors for $T_{0,ITM}$ are as large as 0.16 % for the ideal gas model, but only 0.015 % for the polytropic model.

This manuscript introduces a new model that compensates for real gas effects in high beta ratio ($\beta > 0.25$) CFV installations. Traditional real gas corrections based on C_{JM}^* are accurate at low pressures and for low beta ratio CFV installations ($\beta \leq 0.25$), but introduce errors of nearly 0.4 % at high pressures for $\beta > 0.25$. Herein, we derive the Real Gas Model from the conservation laws, and provide numerical solutions of the real gas correction factor. In this work the Real Gas Model is applied to methane gas since CFVs are increasingly used in high pressure natural gas applications [7-10]. All thermodynamic properties are computed using the REFPROP program [11].² Moreover, the Real Gas Model has been incorporated into the REFPROP program so that CFV end-users can apply the model to user defined gas compositions (wet air, natural gas, etc.) for selected beta ratios and stagnation conditions.

2. MOTIVATION AND APPLICATIONS OF HIGH BETA RATIO CFV INSTALLATIONS

For many years international and domestic standards documents [5, 6] have recommended using CFV installations with $\beta \leq 0.25$. When β values are small, the velocity in the approach piping is low. For example, for methane gas at 295 K, a beta ratio of $\beta = 0.1$ has an approximate velocity of 2.6 m/s. Two advantages of low velocities include 1) a straightforward calculation of

² REFPROP is a NIST-maintained database that calculates thermodynamic and transport properties of natural gas mixtures and other fluids such as water, air, refrigerants, numerous pure gases, etc.

the stagnation temperature, and 2) CFV flow measurements that are nearly immune to velocity profile installation effects. For low velocities, the ITMs accurately predict the stagnation temperature even if real gas effects are significant (see Fig. 2). The acceleration of the low velocity gas to sonic conditions at the CFV throat significantly reduces installation effects due to non-ideal velocity profiles.

On the other hand, it is difficult to measure T_{m1} accurately in slowly moving gases. Nevertheless, the average temperature just upstream of the CFV entrance must be accurately measured for low uncertainty flow measurements. For small flows a heat exchanger is often a practical remedy to ensure a low uncertainty temperature measurement; however, for large flows a properly sized heat exchanger is often too expensive. Moreover, when CFVs are used to measure large flows there are often additional factors that make an already challenging temperature measurement even more difficult. A few examples include 1) blow-down calibrations where a high pressure tank is discharged upstream of a CFV, 2) CFVs installed in large diameter upstream piping where the flowing gas temperature differs from the surrounding environment, 3) CFVs used as working standards to calibrate other CFVs, and 4) calibration of explosive gases (e.g., natural gas) where safety regulations require that temperature probes be installed in thermowells. The first 3 scenarios can result in a temperature field that varies spatially and temporally. Both phenomena can introduce additional uncertainty in the temperature measurement [12, 13]. Likewise, thermowells can also increase the uncertainty of the temperature measurement due to contact resistance and thermal inertia. In these CFV applications a higher velocity in the approach piping would increase convective heat transfer and likely reduce temperature measurement uncertainty. The larger velocity realized by a high beta ratio CFV installation could offset the advantages of a low velocity flow (*i.e.*, low beta ratio) in these scenarios. The Real Gas Model introduced herein accounts for the real gas corrections that are necessary for high beta ratio CFV installations.

3. REVIEW OF THE CFV MASS FLOW MODEL

3.1. Baseline CFV Model

The CFV mass flow model is based on compressible gas dynamic theory assuming 1) that the flow processes are ideal³ and 2) that the gas thermodynamic behavior can be modeled by the ITMs [14, 15]. Under these assumptions the baseline mass flow is

$$\dot{m}_b = \frac{C_{ITM}^* P_{0,ITM} A^* \sqrt{\mathcal{M}}}{\sqrt{R_{univ} T_{0,ITM}}} \quad (1)$$

where $A^* = \pi d^2/4$ is the throat area, \mathcal{M} is the molar mass, $R_{univ} = 8314.471 \text{ J/(kmol}\cdot\text{K)}$ is the universal gas constant [16], and C_{ITM}^* is the critical flow function determined with the ITMs.⁴ The baseline CFV model generally gives results within 5 % (or better) of the actual mass flow. However, if the model is corrected for non-ideal flow phenomena and real gas effects, then low uncertainty mass flow measurements can be realized.

³ Here ideal flow indicates that the flow is one-dimensional (*i.e.*, flat sonic line at throat section) and inviscid.

⁴ Analytical expressions of C_{ITM}^* for the ideal gas model and the polytropic model are given in the Appendix.

3.2. Review of Flow and Real Gas Correction Factors

Composite Linear CFV theory [17] shows that non-ideal flow corrections are independent from real gas effects, and vice versa. That is, the coupling between real gas effects and non-ideal flow physics (*i.e.*, the boundary layer along the CFV wall and multidimensional effects in the core flow) result in second order corrections to the mass flow that are generally negligible relative to other uncertainty sources. As a result the baseline model can be corrected using two independent correction factors, one that corrects for non-ideal flow phenomena and the other that corrects for real gas effects. For the CFV installation shown in Fig. 1, the corrected mass flow model is

$$\dot{m} = C_{d,\text{flow}} C_{d,\text{real}} \dot{m}_b \quad (2)$$

where $C_{d,\text{flow}}$ is the flow discharge coefficient, and $C_{d,\text{real}}$ is the real gas discharge coefficient. The flow discharge coefficient corrects for non-ideal flow phenomena. It accounts for Reynolds number effects associated with the boundary layer along the CFV wall [18] and the curvature of the sonic line at the throat [19]. The real gas discharge coefficient accounts for real gas behavior and is defined by

$$C_{d,\text{real}} = \frac{\dot{M}''_{\text{real}}}{\dot{m}''_b} \quad (3)$$

where \dot{M}''_{real} is the inviscid real gas mass flux, and $\dot{m}''_b = \dot{m}_b / A^*$ is the baseline mass flux. In contrast to $C_{d,\text{flow}}$, which is generally determined experimentally via flow calibration, $C_{d,\text{real}}$ is theoretically determined.

3.3. Real Gas Corrections based on Johnson's Method [4]

In the 1970's Johnson used the best available thermodynamic equation of state and numerically solved for $\dot{M}''_{\text{real,JM}}$ [1]. He calculated the stagnation entropy and stagnation enthalpy based on gas composition, and the stagnation pressure and temperature in the CFV approach piping. His numerical algorithm calculated the temperature and pressure along an isentrope until 1) the value of the local stagnation enthalpy equaled the upstream value, and 2) the Mach number was unity. At the condition of unity Mach number, the product of the density and speed of sound equals the real gas mass flux.

Johnson's real gas model is still the state of the art for correcting real gas behavior in CFV flows. Over the years the numerical algorithm has been improved and the thermodynamic equations of state have become more accurate, but the framework developed by Johnson has remained essentially unchanged. The required inputs for Johnson's model are the gas composition and the stagnation pressure and temperature in the approach piping. His model assumes that all real gas effects can be lumped into the real gas critical flow function (C_{JM}^*). As such, the stagnation pressure ($P_{0,\text{ITM}}$) and temperature ($T_{0,\text{ITM}}$) are based on the ITMs, and these idealized values are used to determine the entropy and stagnation enthalpy in the Johnson model.

When Johnson's numerical solution is depicted in a form analogous to Eqn. (1) the resulting expression for the real gas mass flow is

$$\dot{M}_{\text{real,JM}} = \dot{M}''_{\text{real,JM}} A^* = \frac{C_{\text{JM}}^* P_{0,\text{ITM}} \sqrt{\mathcal{M}} A^*}{\sqrt{R_{\text{univ}} T_{0,\text{ITM}}}} \quad (4)$$

where the real gas critical flow function (C_{JM}^*) is defined by [1]

$$C^* \equiv \frac{\rho^* a^* \sqrt{R_{univ} T_0}}{P_0 \sqrt{\mathcal{M}}} \quad (5)$$

Here ρ^* and a^* are the respective density and speed of sound at the condition of unity Mach number. By combining Eqns. (3) and (4), the contemporary real gas discharge coefficient is

$$C_{d,real,JM} = \frac{\dot{M}''_{real,JM}}{\dot{m}'_b} = \frac{C_{JM}^*}{C_{ITM}^*} \quad (6)$$

the critical flow function developed by Johnson divided by either of the critical flow functions based on the ITMs. The current CFV mass flow model is derived by combining Eqn. (6) with Eqns. (1) and (2) giving

$$\dot{m}_{JM} = C_{d,flow} C_{d,real,JM} \dot{m}_b = \frac{C_{d,flow} C_{JM}^* P_{0,ITM} A^* \sqrt{\mathcal{M}}}{\sqrt{R_{univ} T_{0,ITM}}} \quad (7)$$

where all real gas effects are lumped into C_{JM}^* .

3.4. Real Gas Model (RGM) for High Beta Ratio CFV Applications

Equation (6) is presently the state of the art for correcting real gas effects in CFV flows. As such, thermodynamic software programs have been developed to compute the critical flow function (C_{JM}^*) for a specified gas composition and input stagnation conditions $P_{0,ITM}$ and $T_{0,ITM}$. The use of $P_{0,ITM}$ and $T_{0,ITM}$ is justified at low pressures and in low beta ratio applications ($\beta \leq 0.25$) as evidenced by the good agreement between the RGM and the ITMs shown in Fig. 2. However, the differences between the RGM and ITMs for $\beta > 0.25$ indicate a need for additional real gas corrections for high beta ratio CFV installations. The RGM developed herein is intended to correct for these cases.

The mass flow computed using the Real Gas Model follows the form used for the baseline mass flow model in Eqn. (1) and the contemporary model established by Johnson in Eqn. (4). It is expressed by

$$\dot{m}_{RGM} = \frac{C_{RGM}^* P_{0,RGM} \sqrt{\mathcal{M}} A^*}{\sqrt{R_{univ} T_{0,RGM}}} \quad (8)$$

where $P_{0,RGM}$, $T_{0,RGM}$, and C_{RGM}^* are the stagnation pressure, temperature, and real gas critical flow function calculated by the RGM. We point out that C_{RGM}^* will in general differ from C_{JM}^* even though they are both based on the same definition for the real gas critical function given in Eqn. (5). Their values differ because each is evaluated at different stagnation conditions; C_{JM}^* is evaluated at $P_{0,ITM}$ and $T_{0,ITM}$ while C_{RGM}^* is evaluated at $P_{0,RGM}$ and $T_{0,RGM}$. Figure 2 shows that the stagnation conditions based on the ITMs do not in general agree with the RGM for $\beta > 0.25$. The difference between C_{JM}^* and C_{RGM}^* is shown in Section 5.

In the following sections we present the theoretical basis of the RGM, and derive six coupled, algebraic expressions that comprise the model. These equations must be solved with a low uncertainty thermodynamic equation of state to determine the real gas correction factor. In general, low uncertainty thermodynamic equations of state are too complex to obtain analytical solutions, and a numerical approach is necessary. We outline the numerical method used herein and compare solutions of the RGM with the contemporary model in current use.

4. FORMULATION OF THE REAL GAS MODEL (RGM)

The gas dynamic equations for mass, momentum, and energy conservation are the underlying equations for the RGM. Since real gas effects are unaffected by non-ideal flow physics (*i.e.*, the multi-dimensional core flow and viscous boundary layer adjacent to the wall), the conservation equations are solved for an ideal flow (*i.e.*, one-dimensional and inviscid). For an ideal flow the conservation equations are [20]

$$\dot{M}_{\text{real}} = \rho_x u_x A_x \quad (9a)$$

$$h_0 = h_{t,x} \quad (9b)$$

$$s_0 = s_x \quad (9c)$$

where the subscript “x” indicates any axial location between the approach pipe and CFV throat. Conservation of mass is given by Eqn. (9a), which indicates that the density (ρ_x), velocity (u_x), and cross sectional area (A_x) vary in the x direction so that the real gas mass flow (\dot{M}_{real}) is constant. Equation (9b) is energy conservation, and Eqn. (9c) is a linear combination of momentum and energy. The latter two equations indicate that the flow process is both isoenergetic and isentropic. The isoenergetic and isentropic conditions stipulate that the total enthalpy ($h_{t,x} = h_x + u_x^2/2$) and the entropy (s_x) for any x location are constant, and equal their respective values evaluated at the stagnation conditions.

4.1. Six Coupled Algebraic Equations Comprising the Real Gas Model (RGM)

The conservation laws specified in Eqns. (9a) through (9c) are used to develop five of the equations used in the RGM. The sixth equation is an empirical relationship relating the temperature measured in the approach piping (T_{m1}) to the static temperature (T_1).

Empirical Relationship between the Measured and Static Temperature

The required inputs for the RGM include the measurements of temperature (T_{m1}) and static pressure (P_1) made in the approach pipe shown in Fig. 1, the beta ratio (β), and the recovery factor (R_f). The recovery factor is a dimensionless ratio of temperature differences given by

$$R_f = \frac{T_{m1} - T_1}{T_0 - T_1} \quad (10a)$$

where the numerator is the difference between the measured and static temperature, and the denominator is the difference between the freestream stagnation temperature and the static temperature. As illustrated in Fig. 1 the temperature probe protrudes into the flow stream so that the gas comes to rest against the surface of the probe. As the gas decelerates in the boundary layer adjacent to the probe surface, frictional heating causes the static temperature (T_1) to

increase. At the probe surface where the velocity is zero, the gas temperature increases to T_{m1} . If frictional heating is balanced by conductive losses (*i.e.*, unity Prandtl number, $Pr = 1$) then the process can be considered to be adiabatic and the measured wall temperature equals the freestream stagnation temperature, $T_{m1} = T_0$ [21]. If on the other hand, all of the generated heat is lost to conduction (*i.e.*, Prandtl number approaching zero, $Pr \rightarrow 0$) then $T_{m1} = T_1$. In this way the recovery factor is a function of the Prandtl number (Pr).

Theoretical work has shown that for laminar flow over a flat plate the recovery factor can be approximated by \sqrt{Pr} while for turbulent flow it is $\sqrt[3]{Pr}$. Since most low-density gases have $Pr \approx 0.7$ the recovery factor typically ranges from $R_f = 0.84$ to 0.9 for flow over a flat plate [22]. For a temperature sensor the recovery factor is affected by Pr as well as the probe design, shape, and orientation to the flow. Moffat found that the recovery factor for thermocouple junctions of round wire oriented parallel to the flow were $R_f = 0.86 \pm 0.09$, but decreased to $R_f = 0.68 \pm 0.07$ when oriented perpendicular to the flow [23]. In this work we take $R_f = 0.75$.

Application of Conservation Laws in Deriving the Real Gas Model

The isoenergetic and isentropic conditions specified by Eqns. (9b) and (9c) are applied at the CFV throat, and the resulting expressions are

$$h_0 = h^* + a^{*2}/2 \quad (10b)$$

$$s_0 = s^* \quad (10c)$$

where h^* and s^* are the respective static enthalpy and entropy at the CFV throat. These equations show that the thermodynamic state at the CFV throat is uniquely defined by the upstream stagnation properties. Thus, if we knew the upstream stagnation conditions we could determine ρ^* and a^* , and subsequently the thermodynamic property C^* defined in Eqn. (4).

The isoenergetic and isentropic conditions are applied a second time to relate the stagnation conditions to those in the approach pipe. The resulting expressions are

$$h_0 = h_1 + u_1^2/2 \quad (10d)$$

$$s_0 = s_1 \quad (10e)$$

where h_1 and s_1 are the respective static enthalpy and entropy in the approach pipe. The velocity (u_1) in Eqn. (10d) is strongly coupled to the beta ratio through the conservation of mass in Eqn (9a), which when applied between the approach pipe and CFV throat gives

$$\rho_1 u_1 = \rho^* a^* \beta^2 \quad (10f)$$

where the ratio of the CFV throat area ($A^* = \pi d^2/4$) to the approach pipe area ($A_1 = \pi D^2/4$) is β squared.

4.2. Numerical Solution of the Real Gas Model (RGM)

All thermodynamic properties in Eqns. (10a) through (10f) are evaluated using the REFPROP program [10]. The equations are solved numerically following the 6 step iterative routine shown in Fig. 3. The iterative procedure begins in Step 1 by estimating the stagnation pressure and

temperature by $P_{0,ITM}$ and $T_{0,ITM}$. In Step 2 we solve Eqns. (10b) and (10c) for the throat temperature (T^*) and pressure (P^*) based on the stagnation pressure and temperature from step 1. These two equations are solved numerically using the Secant Method [24]. In Step 2 we also solve Eqn. (10a) for the static temperature in the approach pipe (T_1). Next, in Step 3 we solve Eqn. (10f) for the velocity in the approach pipe (u_1) using the computed values of T^* , P^* , and T_1 . The Secant Method is used a second time in Step 4 to calculate updated values of stagnation pressure (P_0) and temperature (T_0) by solving Eqns. (10d) and (10e). Step 5 compares the updated values of P_0 and T_0 with the values used in Step 1. If the absolute difference of the stagnation pressure (or stagnation temperature) changes by more 0.000001 % between Steps 1 and 4, then another iteration is performed using the updated stagnation values as inputs in Step 1. On the other hand, if the updated values of P_0 and T_0 do not change by more than 0.000001 %, we first verify that Eqns. (10b) and (10c) are satisfied before exiting the iterative loop and calculating the real gas mass flow (\dot{M}''_{real}), the real gas critical flow function (C^*_{RGM}), and the stagnation pressure ($P_{0,RGM}$) and temperature ($T_{0,RGM}$) in Step 6.

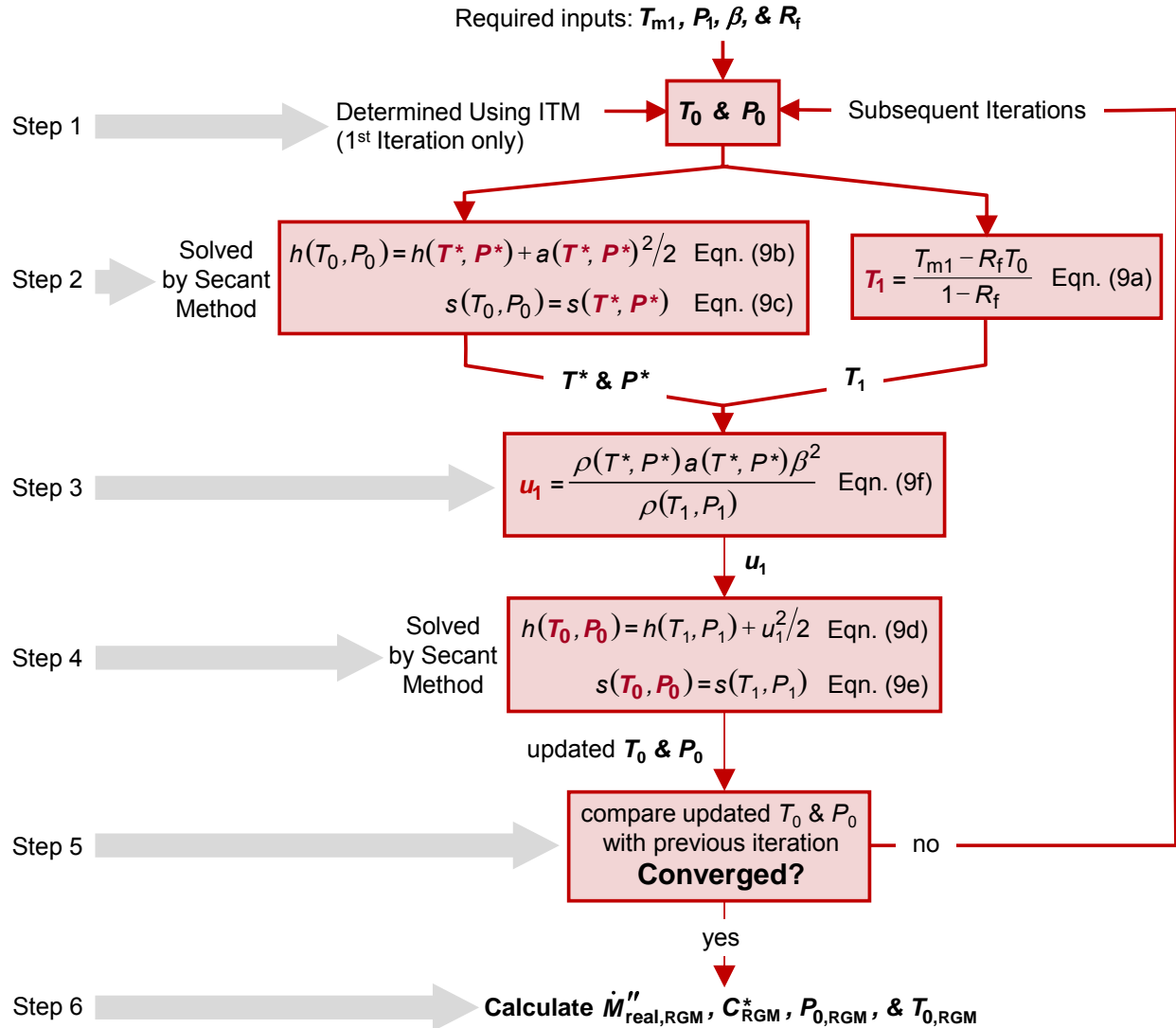


Figure 3. Schematic depicting the iterative scheme used to solve the Real Gas Model. (Thermodynamic properties evaluated using the REFPROP program.)

5. RESULTS

The Real Gas Model (RGM) described in this manuscript is used to assess the error levels of the contemporary model used in the CFV mass flow model. The current model to correct for real gas effects is based on the work of Johnson [1], who lumped all real gas corrections into the real gas critical flow function (C_{JM}^*). This thermodynamic parameter is determined as a function of the stagnation pressure ($P_{0,\text{ITM}}$) and temperature ($T_{0,\text{ITM}}$) based on the ITMs. These parameters are used to determine the real gas mass flow ($\dot{M}_{\text{real},\text{JM}}$) given in Eqn. (4). The errors in the stagnation pressure ($P_{0,\text{ITM}}$) and temperature ($T_{0,\text{ITM}}$) are shown in Fig. 1. In this section we first assess the error of C_{JM}^* followed by the error in $\dot{M}_{\text{real},\text{JM}}$. Results are shown for CFV installations with β values ranging from 0.01 to 0.6. The working fluid is methane gas at 295 K and pressures ranging from 0.1 MPa to 20 MPa.

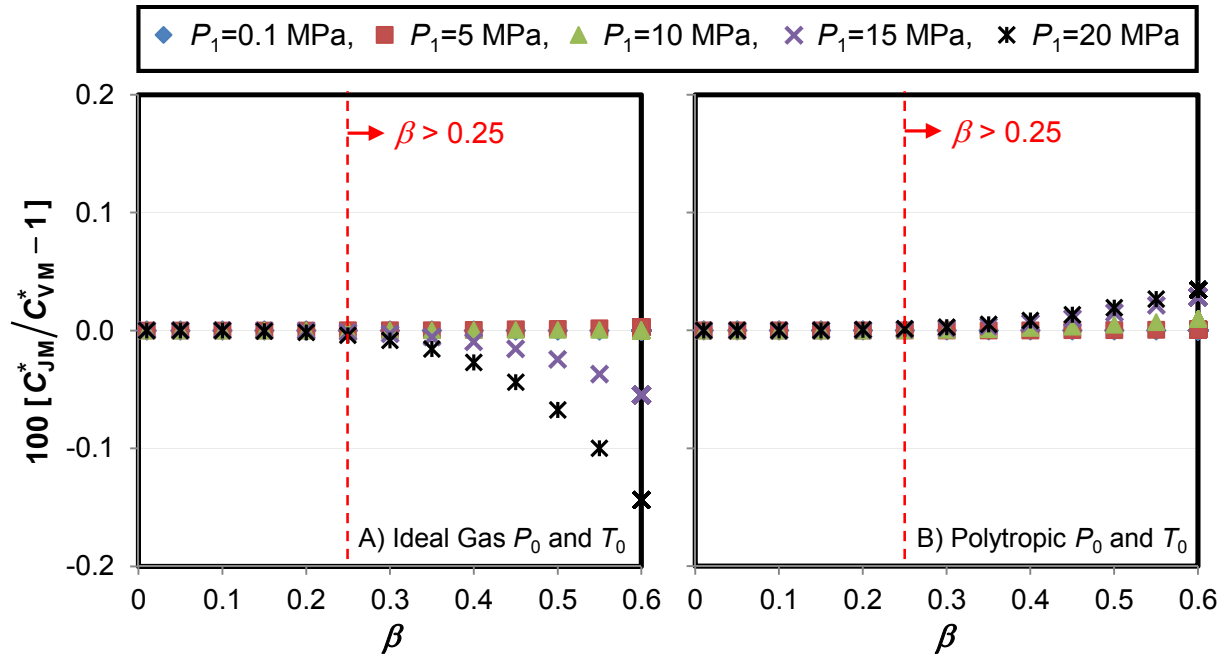


Figure 4. Errors in C_{JM}^* for methane gas at 295 K plotted versus β : A) C_{JM}^* is determined using stagnation pressure and temperature based on the ideal gas model, and B) C_{JM}^* is calculated using stagnation pressure and temperature based on the polytropic gas model.

Figure 4 plots the error in the real gas critical flow function (C_{JM}^*) versus β . Here C_{JM}^* is calculated with the REFPROP program with input stagnation pressure and temperature from the ITMs. In particular, the stagnation conditions were determined based on the ideal gas model in Fig. 4A, and on the polytropic gas model in Fig. 4B.⁵ As expected, the figures show no significant error for $\beta \leq 0.25$. However, Fig. 4A shows increasing errors above 10 MPa for $\beta > 0.25$. Absolute maximum errors are 0.15 % at 20 MPa and $\beta = 0.6$. In contrast, in Fig. 4B the maximum error in C_{JM}^* is less than 0.04 %.

Figure 5 plots the error in the real gas mass flux ($\dot{M}_{real,JM}''$) versus β . As indicated in Fig. 5A the ideal gas stagnation pressure and temperature are used to determine C_{JM}^* , and subsequently $\dot{M}_{real,JM}''$. Similarly, values of $\dot{M}_{real,JM}''$ in Fig. 5B are determined using stagnation pressure and temperature based on the polytropic model. Both Figs. 5A and 5B show negligible error for $\beta \leq 0.25$, thereby demonstrating that the existing real gas model is accurate for low beta ratio CFV installations. However, for $\beta > 0.25$ Fig. 5B shows that the error increases with increasing pressures, reaching a maximum error of nearly 0.4 % at 20 MPa and $\beta = 0.6$. In contrast, the errors in Fig. 5A reach a maximum value of 0.3 % at 10 MPa. At higher pressures the absolute error decreases, and ultimately obtains a value of 0.2 % at 20 MPa.

⁵ Analytic expressions for the ITMs are given in the Appendix.

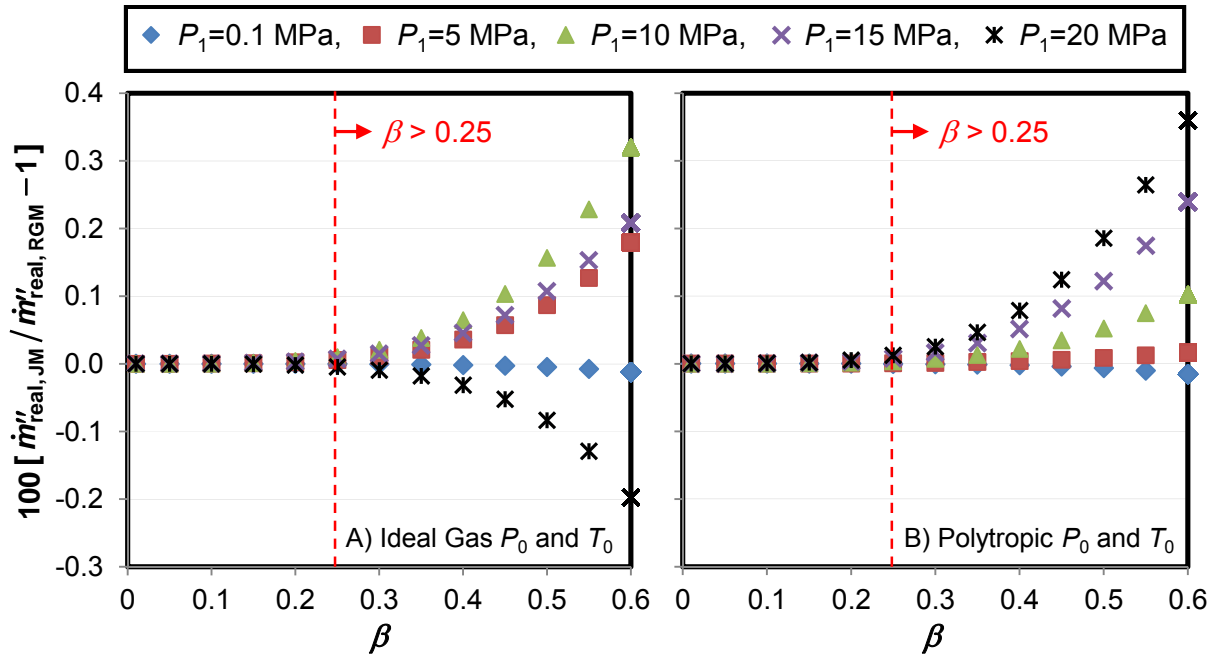


Figure 5. Error in $\dot{m}''_{\text{real, JM}}$ computed using ITMs plotted versus β . (Plots are for methane at 295 K for the 5 pressures ranging from 0.1 MPa to 20 MPa.)

6. CONCLUSIONS

A new real gas model is presented that corrects for real gas effects in high beta ratio ($\beta > 2.5$) CFV installations. The model is derived using the gas dynamics conservation laws, and is solved numerically for CFV installations with beta ratios ranging from 0.1 to 0.6. All thermodynamic properties are determined using the REFPROP program, and solutions of the Real Gas model are given for methane gas at 295 K and pressures up to 20 MPa. The high beta ratio real gas model is used to assess error levels in the contemporary low beta ratio real gas model based on the work of Johnson [1]. As expected, for low beta ratio CFV installations ($\beta \leq 2.5$) both models agree to better than 0.01 %; however, the agreement is not as good at high beta ratios and high pressures. Error levels exceed 0.1 % for $\beta = 0.5$ and a pressure of 10 MPa, and are greater than 0.3 % at $\beta = 0.6$ and a pressure of 20 MPa.

The Real Gas Model introduced herein is programmed into the REFPROP software so that end-users can compute high beta real gas corrections for selected gas compositions, beta ratios, and stagnation conditions.

APPENDIX

Analytical Expressions used in CFV Calculations based on the Idealized Thermodynamic Models (ITMs)

The two idealized thermodynamic models (ITMs) currently used in CFV applications include the following: 1) the ideal gas model for which the gas density is $\rho = \mathcal{M}P/R_{\text{univ}}T$ and the specific heat ratio (γ) is taken to be constant, and 2) the polytropic model for which the density varies with pressure according to $P\rho^{-n} = \text{constant}$ and the isentropic exponent (n) is taken to be

constant.⁶ Researchers have used the ITMs to develop analytical expressions for $P_{0,ITM}$, $T_{0,ITM}$, and C_{ITM}^* [14, 15, 20]. The analytical expressions of $P_{0,ITM}$ and $T_{0,ITM}$ are used both in the baseline mass flow model in Eqn. (1) as well as the inputs to Johnson's method for calculating the real gas critical flow function (C_{JM}^*) [1-4]. In contrast, values of C_{ITM}^* do not generally provide sufficient accuracy for low uncertainty flow measurements and should only be used if real gas effects are insignificant [25]. Nevertheless, for completeness the expression for C_{ITM}^* are included in this Appendix.

Analytic Expressions based on the Polytropic Gas Model

Cornelius [15] solved Eqns. (10d) and (10e) using the polytropic gas model and developed analytic expressions for the stagnation pressure, stagnation temperature, and the critical flow function. The expressions for these parameters are

$$P_{0,p} = P \left[1 + \left(\frac{n-1}{2} \right) Ma_{p1}^2 \right]^{n/n-1} \quad (11a)$$

$$T_{0,p} = T_1 \left[1 + \left(\frac{n-1}{2} \right) Ma^2 \right]^{\kappa} \quad (11b)$$

$$C_p^* = \sqrt{\frac{n}{Z_0} \left(\frac{n+1}{2} \right)^{\frac{1+n}{2(1-n)}}} \quad (11c)$$

where the subscript "p" indicates the polytropic gas model, and $n = n(P_1, T_{m1})$ is the isentropic exponent evaluated using the measured pressure and temperature, and $Z_0 = Z(P_{0,p}, T_{0,p})$ is the compressibility factor evaluated at the stagnation condition pressure and temperature. The exponent on the stagnation temperature is

$$\kappa = \left(\frac{n}{r} \right) \left(\frac{r-1}{n-1} \right) \quad (11d)$$

where the parameter r is defined by

$$r \equiv \left[1 + Z \left(\frac{R_u}{\mathcal{M} c_p} \right) \left(\frac{T \rho_T}{\rho} \right) \right]^{-1} \quad (11e)$$

where Z is the compressibility factor, $\rho_T = [\partial \rho / \partial T]_P$ is the partial derivative of density with respect to temperature at a fixed pressure, and c_p is the specific heat capacity at constant pressure. Cornelius assumed that the grouping of thermodynamic variables defined by r was constant in his analytic expression of the stagnation temperature [15]. This parameter is evaluated at the measured temperature and pressure, $r = r(P_1, T_{m1})$.

⁶ The isentropic exponent is defined by $n \equiv \frac{\rho}{P} \frac{\partial P}{\partial \rho} \Big|_s$ where ρ is the density and the derivative term is the speed of sound squared, $a^2 = [\partial P / \partial \rho]_s$.

The expression for the stagnation temperature given in Eqn. (11b) is not practical for CFV calculations since T_1 is unknown. The equation is combined with Eqn. (10a) so that the stagnation temperature is given in terms of the measured temperature,

$$T_{0,p} = T_{m1} \left(\frac{\left[1 + \left(\frac{n-1}{2} \right) Ma^2 \right]^\kappa}{(1-R_f) + R_f \left[1 + \left(\frac{n-1}{2} \right) Ma^2 \right]^\kappa} \right). \quad (11f)$$

However, instead of using the exact expression given by Eqn. (11f), for convenience, the CFV flow measurement community uses a low Mach number approximation of the stagnation temperature given by

$$T_{0,p} = T_{m1} \left[1 + \kappa (1-R_f) \left(\frac{n-1}{2} \right) Ma^2 \right] \quad (11g)$$

which is accurate to Mach number to the fourth power. A low Mach number approximation is also used to relate the Mach number to β ,

$$Ma_{p1} = \frac{1}{\beta^2} \left(\frac{2}{n+1} \right)^{(n-3)/(2n-2)} \left[1 - \sqrt{1 - 2\beta^4 \left(\frac{2}{n+1} \right)^{2/(n-1)}} \right]. \quad (11h)$$

The exact Mach number relationship [14, 20] is generally inconvenient to use as the Mach number cannot be analytically solved explicitly as a function of β . The approximation in Eqn. (11h) gives Mach number to accuracies better than 0.02 % for $\beta \leq 0.6$ [7].

Analytic Expressions based on the Ideal Gas Model

All of the analytic expressions based on the ideal gas model are derived in the literature [14, 20]. These expressions can also be derived using expressions from the polytropic model. In particular, if we assume that the gas behavior is ideal (*i.e.*, a unity compressibility factor), then $n \rightarrow \gamma$. In this way the polytropic equations simplify to the ideal gas equations by taking $Z = 1$ and $n = \gamma$.⁷ These equations are given here for completeness. The stagnation pressure, temperature, and critical flow function are given by

$$P_{0,i} = P_1 \left[1 + \left(\frac{\gamma-1}{2} \right) Ma_{i1}^2 \right]^{\gamma/\gamma-1} \quad (12a)$$

$$T_{0,i} = T_1 \left[1 + \left(\frac{\gamma-1}{2} \right) Ma_{i1}^2 \right] \quad (12b)$$

$$C_i^* = \sqrt{\gamma} \left(\frac{\gamma+1}{2} \right)^{\frac{1+\gamma}{2(1-\gamma)}} \quad (12c)$$

where the subscript “i” indicates the ideal gas model, $\gamma = \gamma(P_1, T_{m1})$ is the specific heat ratio evaluated using the measured pressure and temperature, and Ma_{i1} is the Mach number in the

⁷ For the ideal gas model the variable r in Eqn. (11e) becomes the specific heat ratio, $r = \gamma$. As a result the exponent defined in Eqn. (11d) equals unity, $\kappa = 1$.

approach pipe. The exact expression for the stagnation temperature expressed as a function of the measured temperature is

$$T_{0,i} = T_{m1} \left[\frac{1 + \left(\frac{\gamma-1}{2} \right) Ma_{i1}^2}{1 + R_f \left(\frac{\gamma-1}{2} \right) Ma_{i1}^2} \right], \quad (12d)$$

and the low Mach number approximation used in the CFV flow measurement community is

$$T_{0,i} = T_{m1} \left[1 + \left(\frac{\gamma-1}{2} \right) (1 - R_f) Ma_{i1}^2 \right], \quad (12e)$$

which is accurate to Mach number to the fourth power.

The Mach number is a function of the beta ratio and the specific heat ratio and is given by

$$Ma_{i1} = \frac{1}{\beta^2} \left(\frac{2}{\gamma+1} \right)^{(\gamma-3)/(2\gamma-2)} \left[1 - \sqrt{1 - 2\beta^4 \left(\frac{2}{\gamma+1} \right)^{2/(\gamma-1)}} \right]. \quad (12f)$$

The exact Mach number relationship [14, 20] is generally inconvenient to use as the Mach number cannot be analytically solved as a function of β . The approximation in Eqn (12d) gives Mach number to accuracies better than 0.02 % for $\beta \leq 0.6$ [7].

REFERENCES

- [1] Johnson, R. C., *Calculations of Real-Gas Effects in Flow through Critical Nozzles*, **Journal of Basic Engineering**, 86, pp. 519 – 526, 1964.
- [2] Johnson, R. C., *Real-Gas Effects in Critical Flow through Nozzles and Tabulated Thermodynamic Properties*, NASA TN D-2565, 1965.
- [3] Johnson, R. C., *Calculations of the Flow of Natural Gas through Critical Flow Nozzles*, **Journal of Basic Engineering**, Transactions of the ASME, 92, 3, pp. 580 – 589, 1970.
- [4] Johnson, R. C., *Real Gas Effects in Flowmetering*, **AIP / ASME / ISA / NBS Symposium for Flow, Its Measurement and Control in Science and Industry**, Pittsburgh, Pennsylvania, USA, pp. 269 – 278, 1971.
- [5] International Standards Organization, *Measurement of Gas Flow by Means of Critical Flow Venturi Nozzles*, ISO 9300:2005(E).
- [6] The American Society of Mechanical Engineers, *Measurement of Gas Flow by Means of Critical Flow Venturi Nozzles*, **ASME MFC-7M**, New York, USA, 1987.
- [7] Johnson A. N., *Natural Gas Flow Calibration Service (NGFCS)*, **NIST Special Publication 250-1801**, National Institute of Standards and Technology, Gaithersburg, MD, 2008.
- [8] Johnson, A. N. and Johansen, B., *U.S. National Standards for High Pressure Natural Gas Flow Measurement*, **Proc. of the 2008 Measurement Science Conference**, Anaheim, CA, 2008.
- [9] Mickan, B., Kramer, R., Dopheide, D., Hotze, H., Hinze, H., Johnson, A. N., Wright, J., Vallet, J.-P., *Comparisons by PTB, NIST, and LNE-LADG, in Air and Natural Gas with Critical Venturi Nozzles Agree within 0.05 %*, **Proceedings of the International Symposium on Fluid Flow Measurement**, Queretaro, Mexico, 2006.

-
- [10] Johnson, A. N. and Kegel, T., *Uncertainty and Traceability for the CEESI Iowa Natural Gas Facility*, **J. Res. Natl. Inst. Stand. Technol.**, 109, 345-369, (2004).
- [11] Lemmon, E. W., Huber, M. L., McLinden, M. O., *NIST Standard Reference Database 23: Reference Fluid Thermodynamic and Transport Properties REFPROP, Version 9.1*, **National Institute of Standards and Technology, Standard Reference Data Program**, Gaithersburg, MD, 2013.
- [12] Wright, J. D., Kang, W., Zhang, L., Johnson, A. N., and Moldover, M. R., *Thermal Effects on Critical Flow Venturis*, **9th International Symposium on Fluid Flow Measurement**, Arlington, VA, April 2015.
- [13] Johnson, A. N., Harman, H., and Boyd, J., *Blow-Down Calibration of a Large 8 Path Ultrasonic Flow Meter under Quasi-Steady Flow Conditions*, **The 16th International Flow Measurement Conference FLOMEKO**, Paris, Sept. 2013.
- [14] John, J. E., *Gas Dynamics 2nd Ed.*, **Allyn and Bacon**, Boston MA, 1984.
- [15] Cornelius, K. C., and Srinivas, K., *Isentropic Compressible Flow for Non-Ideal Gas Models for a Venturi*, **J. Fluids Eng.**, 126(2), pp. 238-244, 2004.
- [16] Moldover, M. R., Trusler, J. P. M., Edwards, T. J., Mehl, J. B., and Davis, R. S., *Measurement of the Universal Gas Constant R Using a Spherical Acoustic Resonator*, **J. Res. Natl. Inst. Stand. Technol.**, 93, 2, pp. 85-143, 1988.
- [17] Johnson, A. N. and Wright, J. D., *Comparison Between Theoretical CFV Flow Models and NIST's Primary Flow Data in the Laminar, Turbulent, and Transition Flow Regimes*, **ASME Journal of Fluids Eng.**, Vol. 130., July 2008.
- [18] Tang, S., *Discharge Coefficients for Critical Flow Nozzles and Their Dependence on Reynolds Numbers*, **Ph.D. Thesis, Princeton University**, Princeton, NJ, 1969.
- [19] Kliegel, J. R., and Levine, J. N., *Transonic Flow in Small Throat Radius of Curvature Nozzles*, **AIAA J.**, 7, pp. 1375-1378, 1969.
- [20] Anderson, J. D., *Modern Compressible Flow with Historical Perspective*, **McGraw-Hill Series in Mechanical Engineering**, NY, 1982.
- [21] White, F., *Viscous Fluid Flow 2nd Ed.*, **McGraw-Hill Inc.**, NY, 1991.
- [22] Schlichting, H., *Boundary-Layer Theory 7th Ed.*, **McGraw-Hill Book Company**, NY, 1979.
- [23] Moffat, R. J., *Gas Temperature Measurements*, **Temperature: Its Measurement and Control in Science and Industry**, Vol. 3, Part 2, Reinhold, NY, 1962.
- [24] Press, W. H., Flannery, B. P., Teukolsky S. A., and Vetterling, W. T., *Numerical Recipes*, **Cambridge University Press**, NY, 1989.
- [25] Johnson, A. N., and Johansen, B., *Comparison of Five Natural Gas Equations of State Used for Flow and Energy Measurement*, **7th International Symposium on Fluid Flow Measurement**, Anchorage, AK, 2009.